Acta Crystallographica Section D
Biological Crystallography
ISSN 0907-4449

α-L-Iduronidase forms semi-crystalline spherulites with amyloid-like properties

Laura Ruth, David Eisenberg* and Elizabeth F. Neufeld

Department of Biological Chemistry and Molecular Biology Institute, University California Los Angeles, Los Angeles, CA 90095, USA

Correspondence e-mail: david@mbi.ucla.edu

Received 2 July 1999
Accepted 5 January 2000

While seeking conditions for single crystals of human α-L-iduronidase, solutions were discovered (pH 3.0–8.5 containing calcium or zinc salts) that transform soluble α-L-iduronidase to a solid aggregate. This aggregate is a spherulite of semi-crystalline protein. The X-ray diffraction pattern and ability to bind Congo red characterize the α-L-iduronidase spherulite as 'amyloid-like', in that it displays two of the characteristics of amyloidogenic proteins. In addition, α-L-iduronidase also interacts with heparin, as do some amyloid-forming proteins.

1. Introduction

Amyloid deposits are found in many medical conditions, including familial mediterranean fever, rheumatoid arthritis, Alzheimer's disease, familial amyloid polyneuropathy, adult-onset diabetes, multiple myeloma and primary light-chain-associated amyloidosis (Jiang *et al.*, 1997; Sipe, 1992). These insoluble fibrilar deposits are made up of polymerized proteins, including immunoglobulin monoclonal light chains, transthyretin, β2-microglobulin, lysozyme variants and apolipoprotein A. These proteins have unrelated sequences and three-dimensional structures, which makes the mechanism of amyloid formation a difficult problem to solve (Carrell & Gooptu, 1998). A typical amyloid fibril is 7.5–10 nm wide, of indefinite length, rigid, linear, nonbranching and stainable with Congo red yielding a green birefringence (Puchtler *et al.*, 1962; Burke & Rougvie, 1972). Fibrils often associate with heparin and other glycosaminoglycans, but it is unclear if polysaccharide is necessary for development or stabilization of amyloid fibrils. In any case, some amyloids can be formed *in vitro* in the absence of carbohydrate.

α-L-Iduronidase (E.C. 3.2.1.76) is a lysosomal enzyme that participates in the degradation of the glycosaminoglycans dermatan sulfate and heparan sulfate. In the absence of α-L-iduronidase, partially degraded glycosaminoglycans accumulate in the lysosomes of tissues (Neufeld & Muenzer, 1989). Although amyloid deposits are not part of the pathology in α-L-iduronidase deficiency disease (mucopolysaccharidosis I), α-L-iduronidase forms amyloid-like aggregates. The enzyme has affinity for heparin, as shown by its adherence to heparin-Sepharose columns (Shapiro *et al.*, 1976; Sando & Neufeld, 1977; Kakkis *et al.*, 1994), like several other amyloidogenic proteins (Watson *et al.*, 1997; Bush, Pettingell, Multhaup *et al.*, 1994; Bush, Pettingell, de Paradis *et al.*, 1994; Small *et al.*, 1994; Li *et al.*, 1994; Multhaup *et al.*, 1992; Hamazaki, 1987).

2. Materials and methods

2.1. α-L-Iduronidase spherulites.

Recombinant human α-L-iduronidase was kindly provided by Dr E. Kakkis. The enzyme, made from secretions of an overexpressing Chinese hamster ovary cell line (Kakkis *et al.*, 1994), is currently used for the production of large quantities of α-L-iduronidase for enzyme-replacement therapy (Kakkis *et al.*, 1998). The enzyme, observed as a single band on an SDS–PAGE gel and conservatively estimated to be about 95% pure based on finding only one N-terminus in a similar preparation of enzyme, was stored in buffer (10 m*M* Na_2PO_4 pH 5.8–6.0, 150 m*M* NaCl; preparation *A*). A portion of preparation *A* was further purified using a TosoHaas G3000SWxL (silica) HPLC column and 10 m*M* Na_2PO_4, 150 m*M* Na_2SO_4 pH 5.8 as the elution buffer (preparation *B*). All solutions used for crystallization were sterile filtered. Samples of both preparation *A* and preparation *B* enzyme were dialyzed into 10 m*M* MES or 10 m*M* sodium cacodylate pH 6.0, 150 m*M* NaCl ('start buffer') before crystallization. Spherulites were produced by mixing 1 µl of 2–8 mg ml^{-1} α-L-iduronidase in start buffer with one of several precipitating buffers. Preparation *A* spherulites were obtained by mixing protein in precipitating conditions of 10–24% polyethylene glycol 8000, 100 m*M* buffer pH 3.0–8.5 (such as imidazole, MES, sodium cacodylate, sodium formate or Tris–HCl), a minimum of 10 m*M* calcium salt ($CaCl_2$ or calcium acetate) or 5 m*M* zinc salt ($ZnCl_2$ or zinc acetate) and Na_2PO_4, in a ratio of 2:1:1 (protein:phosphate:precipitant) at 277 and 298 K. In addi-

Table 1
α-L-Iduronidase spherulite formation: detailed ionic composition of screening solutions.

Protein	pH	Buffer	Precipitant	Salt	Concentration (m*M*)	Phosphate	Concentration (m*M*)	Spherulite
Prep. *A*	6.5	Na cacodylate	20% PEG 8K	$CaCl_2$, CaOAc	5–10	None	2.5	−
				$CaCl_2$, CaOAc	5–10	Na_2PO_4	2.5	+
				$CaCl_2$, CaOAc	10	$C_3H_7O_6PNa_2$	2.5	−
				$ZnCl_2$, ZnOAc	5	Na_2PO_4	2.5	+
				$CuCl_2$	200	Na_2PO_4	2.5	−
				$MgCl_2$	200	Na_2PO_4	2.5	−
Prep. *B*	4.6	NaOAc	30% MPD	$CaCl_2$, CaOAc	20	None	n/a	+
				$CaCl_2$, CaOAc	20	Na_2PO_4	n/a	−
	7.5	HEPES	28% PEG 400	$CaCl_2$, CaOAc	200	None	n/a	+
				$CaCl_2$, CaOAc	200	Na_2PO_4	2.5	+
	4.6	NaOAc	20% 2-propanol	$CaCl_2$, CaOAc	200	None	n/a	+
				$CaCl_2$, CaOAc	200	Na_2PO_4	n/a	−
				$ZnCl_2$, ZnOAc	200	None	n/a	+

tion to the PEG/phosphate crystallization condition, preparation *B* spherulites form under a variety of different conditions from Hampton Screens (Jancarik & Kim, 1991; Cudney *et al.*, 1994): (i) 30% MPD, sodium acetate pH 4.6, 20 m*M* $CaCl_2$; (ii) 28% PEG 400, HEPES pH 7.5, 200 m*M* $CaCl_2$; (iii) 20% 2-propanol, sodium acetate pH 4.6, 200 m*M* $CaCl_2$. The spherulites were grown in a hanging-drop experiment apparatus at 277 and 298 K. Copper and magnesium could not replace the calcium or zinc salts. In addition, sodium glycerophosphate could not be substituted for sodium phosphate (Table 1).

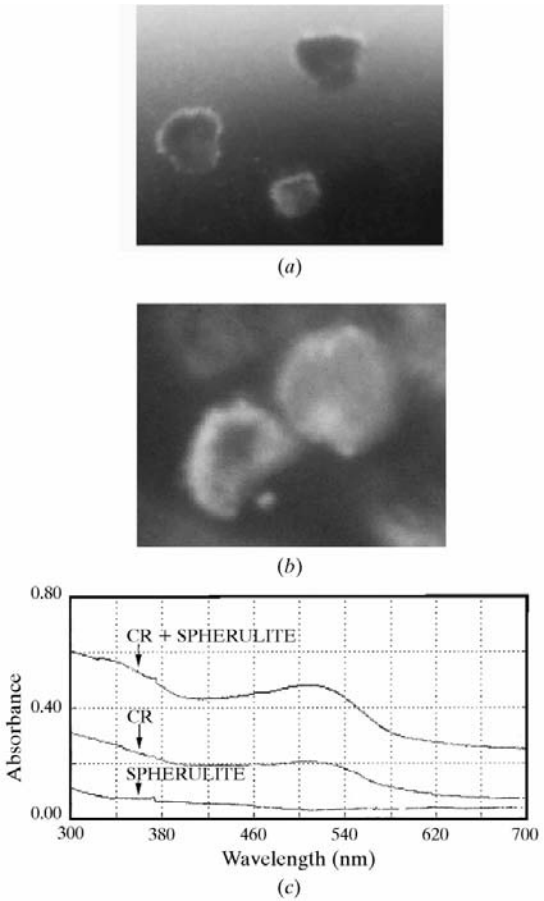

Figure 1
(*a*) α-L-Iduronidase spherulites, unstained (10 µm diameter). (*b*) α-L-Iduronidase spherulite, stained with Congo red (CR). (*c*) UV–VIS wavelength spectrum from 300–700 nm of CR in the absence and presence of approximately 10 µ*M* spherulite. The upper scan represents increased absorbance of CR between 460–500 nm in the presence of spherulite that is characteristic of CR binding to amyloidogenic fibrils.

2.2. Methyl violet staining

α-L-Iduronidase spherulites were washed three times with fresh mother liquor and stained with methyl violet using the method noted by McPherson (1982).

2.3. X-ray diffraction

α-L-Iduronidase spherulites were mounted in 0.5–0.7 m*M* diameter lithium-glass capillary tubes using standard crystal mounting and drying procedures. The diffraction patterns for all spherulite conditions were collected on an R-AXIS IIC image-plate system using nickel-filtered Cu *Kα* radiation (λ = 1.54 Å). Indexing of diffraction data was attempted by hand and with the program *MelB*2000 (Grothe, 1999). *MelB*2000 computes the Bragg plane spacings for a crystal with given unit-cell lengths and angles, where the spacing between planes is inversely related to the radius of the observed ring.

2.4. Congo red staining

α-L-Iduronidase spherulites were stained with Congo red using the methods of Klunk *et al.* (1989*a*,*b*). Using a 0.1% Congo red solution in distilled H_2O, the spherulite staining was determined qualitatively by eye to be orange. The Congo red stained spherulites were also examined using a polarizing microscope. The UV–VIS (λ = 1.54 Å) wavelength spectrum of 2 µ*M* Congo red (in PBS) from 300–700 nm was monitored in the presence and absence of spherulites derived from 10 µ*M* monomer. Six wells of spherulite were washed three times with fresh mother liquor before putting the spherulites into a 2 µ*M* Congo red solution to be used in the spectrophotometer and letting the spherulites stain overnight in the Congo red solution. The amount of Congo red bound to the spherulites was quantified using the method of Klunk *et al.* (1989*a*,*b*).

3. Results

3.1. Spherulite formation

During the process of screening for crystallization conditions for preparation *A* and preparation *B* recombinant human α-L-iduronidase, we discovered aggregates of the enzyme in the form of spherulites in various precipitating conditions. (Preparation *B* was obtained by purifying a sample of preparation *A* by size-exclusion column chromatography.) As was observed for preparation *A* and preparation *B* α-L-iduronidase, it is common in crystallization for different batches of enzyme to yield spherulites under similar and different conditions owing to microscopic batch variations which affect the nucleation process (McPherson, 1982). The α-L-iduronidase spherulite absorbed methyl violet dye and appeared blue–violet, which indicates the spherulite contains protein.

The X-ray diffraction pattern and Congo red staining of the α-L-iduronidase spherulite it suggest that it is 'amyloid-like'. The α-L-iduronidase spherulites formed in 1–5 d at 277 K (Figs. 1*a* and 1*b*) and varied between 10 and 250 µm in diameter. When the α-L-iduronidase spherulites stained with Congo red were examined with a polarizing microscope, they did not birefringe as do classic amyloid structures. Figs. 1(*a*) and 1(*b*), respectively, show the qualitative and quantitative staining of the α-L-iduronidase spherulites with Congo red. The spherulites used for the staining experiment were grown at 277 K. (Spherulites grown at 298 K were also stained; these are not show in the figure.) In Fig. 1(*c*), the entire UV–VIS wavelength spectrum of Congo red between 300–700 nm is observed to shift. The absorbance peak between 460 and 500 nm is more pronounced in the presence of spherulites.

The increased absorbance of the 460–500 nm peak of Congo red plus α-L-iduronidase spherulites is similar to the increase in absorption observed when Congo red binds to insulin fibrils (Klunk *et al.*, 1989*a*,*b*). The spectrum of α-L-iduronidase spherulites alone rules out the possibility that the increased absorption of the Congo red arises from light scattering of the spherulite. From the absorbance, the concentration of bound Congo red is calculated to be 1.6×10^{-6} *M*.

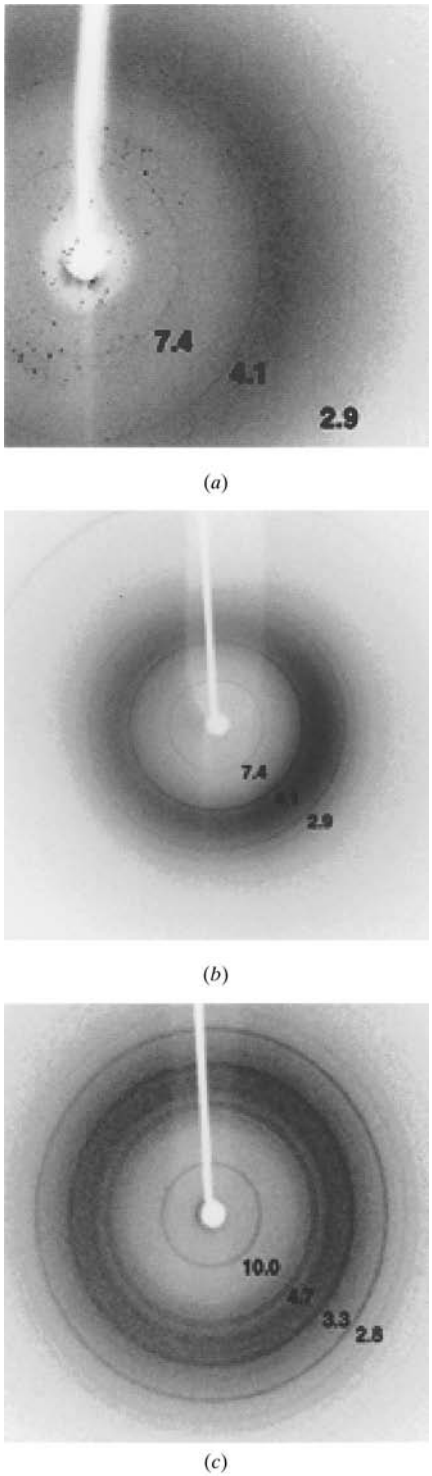

Figure 2
(*a*) X-ray diffraction of a spherulite showing both crystal and powder diffraction. (*b*) X-ray diffraction of a calcium α-L-iduronidase spherulite showing only powder-like ring diffraction. (*c*) X-ray diffraction of zinc α-L-iduronidase spherulite showing only powder-like ring diffraction.

3.2. X-ray diffraction.

The X-ray diffraction patterns of α-L-iduronidase spherulites display both reciprocal-lattice reflections and rings of diffraction at resolutions 10.0–1.9 Å^{-1}. One specimen of α-L-iduronidase spherulites from a single crystallization well yielded diffraction patterns displaying both reciprocal-lattice reflections and rings; the remaining spherulites yielded diffraction patterns displaying only rings. Sample diffraction patterns of the calcium and zinc α-L-iduronidase spherulites are shown in Figs. 2(*a*), 2(*b*) and 2(*c*) and the ring spacings (Å^{-1}) are reported in Table 2. The α-L-iduronidase spherulite diffraction pattern, which has both rings and reciprocal-lattice reflections, may represent a mixed semi-crystalline physical state (Fig. 2*a*). Multiple calcium and zinc α-L-iduronidase spherulites were tested for diffraction and yielded reproducible diffraction patterns.

Although the X-ray diffraction rings of the α-L-iduronidase spherulite are reminiscent of the powder diffraction rings of salts, the reciprocal-lattice spacings of the calcium and zinc α-L-iduronidase are not the same as various salts of these cations. The α-L-iduronidase powder diffraction rings were compared with various salts, such as calcium acetate, calcium chloride, calcium phosphate, calcium sulfate, zinc acetate, zinc chloride, zinc phosphate and zinc sulfate in the Powder Diffraction File 1995, PDF-2 Database Sets 1–45 (Table 2). Sample diffraction rings of $Ca(OH)_2$ and $Zn(OH)_2$ controls, which do not have the same diffraction rings, are given in Table 2. Our attempts to index the α-L-iduronidase spherulite rings with the *MelB*2000 program, as can be done with the diffraction patterns of single crystals, including salts such as $Ca(OH)_2$ and $Zn(OH)_2$, were unsuccessful (Phillips, 1962) because there are insufficient data to provide a unique and accurate solution.

3.3. Comparison with fiber diffraction

The X-ray diffraction rings of our 'amyloid-like' spherulites can be compared with the fiber diffraction data characteristic of classic amyloid fibrils from amyloid-forming proteins (Table 2). Four *ex vivo* amyloid fibrils are listed in Table 2: V30M variant transthyretin (ATTR1), monoclonal λ immunoglobulin light chain (AL), L60R variant apolipoprotein A-I (AapoAI) and A-strand peptide of WT human transthyretin (FTTR). These proteins share with each other some of the meridional reflections at 4.8 and/or 4.7 and/or 4.6, 4.1, 2.9, 2.8, 2.5, 2.3 and 2.1 Å^{-1}, and rings in the equatorial reflections at 8.9 and 10.0 Å^{-1}. The only common meridional reflection found in the previously published classic amyloid fibril data of Sunde *et al.* (1997) is 4.6 Å^{-1}. The purpose of Table 2 is to show that there is a wide variety of meridional and equatorial reflections for previously characterized amyloidogenic proteins. The calcium- and zinc-induced spherulite reflections fall within the range of the tabulated amyloidogenic fibril data. The zinc-induced α-L-iduronidase spherulite does have rings at 10.0 and 4.7 Å^{-1} which are considered characteristic of 'cross-β' structure. The reflections of the α-L-iduronidase spherulites, like those of salts, are sharp rings characteristic of microcrystals, while the reflections of amyloids tend to be diffuse. The spherulites lack the low-angle reflections which are characteristic of long-range order, but otherwise display reflections that tend to correspond to spacings seen in the amyloid fibers and not in the salts. The calcium α-L-iduronidase spherulite shares reflections with the amyloidogenic proteins at 4.1, 2.9, 2.8, 2.3 and 2.1 Å^{-1}, while the zinc α-L-iduronidase spherulite shares reflections with the amyloidogenic proteins at 10.0, 8.9, 4.7, 4.4 and 3.9 Å^{-1}.

4. Discussion

The semi-crystalline metal-specific morphology of our α-L-iduronidase spherulites can be classified as a non-fibrillar 'amyloid-like aggregate'. These X-ray diffraction patterns demonstrate that the α-L-iduronidase spherulites share some features of the classic amyloidogenic cross-β structure fibril diffraction pattern (Sunde *et al.*, 1997; Klunk *et al.*, 1989*a*,*b*; Burke & Rougvie, 1972).

Although we draw a distinction between classic amyloid fibrils and amyloid-like aggregates, a range of amyloid-like aggregates exist. Less ordered fibril and non-fibril amyloid-like aggregates have been observed in other protein systems: (i) the fibril of an SH3 domain (Guijarro *et al.*, 1998), (ii) the amylin amyloid-like aggregate (Moriarty & Raleigh, 1999) and (iii) the non-fibril aggregates observed for both Aβ (Wood *et al.*, 1996) and (iv) the monoclonal immuno-

Table 2
X-ray reflections ($Å^{-1}$) for known amyloidogenic fibrils *versus* α-L-iduronidase spherulites.

Notice that the spherulites lack low-angle reflections, but display reflections which tend to correspond to spacings seen in the amyloid fibers and not in the salts. (E) = equatorial, (M) = meridional

AapoAI†	AL†	ATTR1†	FTTR†	Iduronidase‡		Salt control‡		Salt control§			
				Ca	Zn	Ca(OH)	$Zn(OH)_2$	$CaSO_4$	$ZnSO_4$	CaAc	ZnAc
			26.3 (E)								
15.17 (E)		16.0 (E)					16.8				
		12.60 (E)									
	12.55 (E)										
11.78 (E)			11.51 (E)				10.6			10.8	
		10.10 (E)			10.0					10.3	
9.79 (E)	9.70 (E)									9.8	
			8.92 (E)		8.9						
							8.6				
7.56 (E)	7.56 (E)									7.8	7.5
					7.4						
							6.6			6.4	
	6.11 (E)									6.3	
5.98 (E)		6.05 (E)								5.97	
			5.72 (E)				5.7		5.88		
5.37 (E)		5.32 (E)					5.3		5.48	5.45	
	5.26 (E)									5.18	
	4.82 (M)	4.84 (M)	4.80 (M)			4.9				4.92	
4.79 (M)					4.7						
4.64 (M)	4.62 (M)	4.64 (M)									
			4.58 (M)								4.55
			4.53 (E)								
4.42 (M)					4.4					4.47	
					4.3			4.38		4.25	4.22
					4.2					4.15	
4.12 (M)	4.13 (M)	4.11 (M)		4.1						4.07	4.02
	3.94 (E)				3.9				3.97	3.92	
3.88 (M)	3.85 (M)	3.83 (M)							3.84	3.82	
3.73 (M)		3.71 (M)							3.79	3.68	3.68
	3.61 (M)									3.57	
3.40 (M)			3.43 (E)							3.53	
			3.21 (M)		3.3					3.48	3.46
3.13 (M)									3.14	3.34	
						3.0	3.0	3.0	3.03	3.27	3.28
2.90 (M)				2.9					2.92	3.13	3.12
			2.82 (M)	2.8	2.8				2.73	3.07	
			2.61 (M)			2.6	2.6			2.98	2.90
				2.5	2.5			2.5	2.53		2.50
	2.41 (M)					2.4					2.39
2.39 (M)			2.39 (M)	2.3					2.30		2.29
	2.27 (M)		2.25 (M)					2.2	2.23		2.20
2.17 (M)				2.1				2.1	2.13		2.12
2.00 (M)			2.00 (M)						2.01		2.06
											2.01

† Fibrils: AapoAI, L60R variant apolipoprotein A; AL, monoclonal l immunoglobulin light chain; ATTR1, V30M variant transthyretin; FTTR, peptide with the sequence of the A-strand of wild-type human transthyretin (Sunde *et al.*, 1997). ‡ Data taken from this work. § Data taken from Powder Diffraction File 1995, PDF-2 Database Sets 1–45.

globulin light chain (Helms & Wetzel, 1996). It has been noted that the amyloid fibril formed by an SH3 domain is less ordered than other protein system fibrils because the diffraction pattern includes two rings at 9.4 and 4.7 $Å^{-1}$, no low-angle reflections and has neither an equatorial nor a meridional direction (Guijarro *et al.*, 1998). Similarly, the α-L-iduronidase spherulites may not display lower angle reflections because they lack the long-range order of some other protein system fibrils. Interestingly, there are three other proteins in the literature that form amyloid-like aggregates which stain with Congo red and do not birefringe: (i) SH3 domain (Guijarro *et al.*, 1998), (ii) the κ V_L REI sequence variant D82I domain (Helms & Wetzel, 1996) and (iii) the Alzheimer's amyloid peptide Aβ at pH 5.8 (Wood *et al.*, 1996). In addition, although Moriarty & Raleigh (1999) do not classify aggregated amylin peptide mutant fragments as non-fibril amyloid-like aggregates, the amylin peptide is a major constituent of amyloid deposits seen mainly in islets of type 2 diabetic humans and diabetic cats (Westermark *et al.*, 1990), and the amylin peptide mutant fragments aggregates stain with Congo red (Moriarty & Raleigh, 1999).

The concentration of bound Congo red is calculated from the absorbance to be 1.6×10^{-6} *M*. Since the value of 1.6×10^{-6} *M* is between the Congo red binding characterized for insulin, poly-L-lysine, poly-L-serine and poly-L-lysine at 10^{-7} *M* and thioflavins at 10^{-5} *M*, the Congo red binding to α-L-iduronidase spherulites can be classified as moderate. Since the native soluble α-L-iduronidase protein is predicted to be an (α/β)-barrel (Durand *et al.*, 1997), a cross β-sheet might form in the iduronidase spherulite because of partial denaturation or unfolding of the native soluble α-L-iduronidase protein.

The α-L-iduronidase spherulites form in the presence of metals and it is interesting to compare the metals which help form α-L-iduronidase spherulites and metals which play a role in other amyloidogenic proteins. Five different divalent cations have been shown to cause aggregation or amyloidosis in at least one protein system (Heegaard *et al.*, 1996; Li *et al.*, 1994; Nielsen *et al.*, 1994; Hamazaki, 1987; Pepys & Butler, 1987; Baltz *et al.*, 1982; Table 3). The SAP protein at 100–200 nm concentration specifically aggregates in the presence of 2–25 m*M* calcium in phosphate buffer, which yields a protein:metal ion ratio of 1:20–250. Like SAP, α-L-iduronidase spherulites form in approximately the same concentration range of calcium and not copper, cobalt or magnesium, but unlike SAP the α-L-iduronidase spherulites also form in the presence of zinc. It has been shown that α-L-iduronidase will form dimers in low ionic strength buffers (Barton & Neufeld, 1971). The increase in metal ions in the crystallization buffer may facilitate the aggregation and partial denaturation of protein, which is proposed to be necessary for the formation of an amyloidogenic aggregate of a protein (Liu *et al.*, 1998; Bennett *et al.*, 1995). The crystallization experiments in this paper do not distinguish between the metals causing or promoting α-L-iduronidase spherulite formation.

It may be noteworthy that α-L-iduronidase has an affinity for heparin, as shown by its adherence to heparin Sepharose columns (Shapiro *et al.*, 1976; Sando & Neufeld, 1977; Kakkis *et al.*, 1994), like some of the amyloidogenic proteins, APP, APLP1, APLP2 and SAP, and to briefly compare the potential heparin-binding sites. The recent crystal structure of the N-terminal growth-factor-like domain of Alzheimer amyloid precursor protein reveals that the highly charged basic surface proposed to bind to glycosaminoglycans in the brain is adjacent to a hydrophobic surface which is conserved across the APP family. The hydrophobic surface may play a role in one or more possible functions in the process of forming amyloids, which include carbohydrate binding, metal binding and dimerization interface. The heparin-binding surface in APP is dominated by a loop created by amino-acid residues 96–110, where there is an arginine- and lysine-rich sequence

Table 3
Divalent cations which cause aggregation or amyloid formation in at least one protein system.

Protein	Ion	Ionic concentration (m*M*)
SAP	Ca^{2+}	<1.0
βA4	Zn^{2+}	0.3
PN-2†	Zn^{2+}	0.1
PN-2	Cu^{2+}	0.1
PN-2	Co^{2+}	0.1
APP	Zn^{2+}	0.1
APP	Cu^{2+}	0.1
APP	Co^{2+}	0.1

† PN-2, protease nexin-2.

between amino acids 97–107, CKRGRKQCKH (Rossjohn *et al.*, 1999; Small *et al.*, 1994). Since heparin is known to bind to lysine and arginine motifs, one of the consensus sequences for a heparin-binding site, *XBBXBX* (*X* = hydrophobic residue, *B* = basic residue; Margalit *et al.*, 1993; Jackson *et al.*, 1991; Cardin & Weintraub, 1989), can be used to predict a heparin-binding site in human, canine and murine α-L-iduronidases, FRRMRX, from residues 501–506, 500–505 and 491–496, respectively (Scott *et al.*, 1991; Stoltzfus *et al.*, 1997; Clarke *et al.*, 1994). Since it has been shown that Congo red and heparin share the same binding site in Aβ, it is possible that Congo red binds to the heparin-binding site in the α-L-iduronidase spherulites (Watson *et al.*, 1997; Caughey *et al.*, 1994).

In conclusion, α-L-iduronidase seems to specifically sequester the divalent cations calcium and zinc to form micro-crystalline spherulites and it is interesting that other amyloidogenic proteins, such as SAP and Ab, also sequester the metal ions calcium and zinc, respectively. The X-ray diffraction pattern and Congo red staining of the α-L-iduronidase spherulite characterize it as amyloid-like. This adds another protein to the list of non-homologous proteins that undergo a conformational change to form the characteristic cross-β structure observed in amyloidogenic fibrils. Future structural and biochemical studies may help to elucidate the mechanism of conformational change in α-L-iduronidase as well as other amyloidogenic proteins and to relate the structures of these amyloid-like spherulites to classic amyloid fibrils.

We thank NIH for support and Dr E. Kakkis for the gift of recombinant α-L-iduronidase protein. Dr E. Kakkis' previous affiliation was Division of Medical Genetics, Department of Pediatrics, Harbor-UCLA Medical Center, Torrance, CA 90502, USA, and current affiliation is BioMarin Pharmaceutical, Inc., Novato, CA 94949, USA. LR is a trainee of the UCLA Intercampus Medical Genetics Program supported by NIH Medical Genetics Training Grant GM08243.

References

Baltz, M. L., De Beer, F. C., Feinstein, A. & Pepys, M. B. (1982). *Biochim. Biophys. Acta*, **701**, 229–236.

Barton, R. & Neufeld, E. F. (1971). *J. Biol. Chem.* **246**, 7773–7779.

Bennett, M. J., Schlunegger, M. P. & Eisenberg, D. S. (1995). *Protein Sci.* **4**, 2455–2468.

Burke, M. J. R. & Rougvie, M. A. (1972). *Biochemistry*, **11**, 2435–2439.

Bush, A. I., Pettingell, W. H. Jr., de Paradis, M., Tanzi, R. E. & Wasco, W. (1994). *J. Biol. Chem.* **269**(43), 26618–26621.

Bush, A. I., Pettingell, W. H., Multhaup, G., de Paradis, M., Vonsattel, J.-P., Gusella, J. F., Beyreuther, K., Masters, C. L. & Tanzi, R. E. (1994). *Science*, **265**, 1464–1467.

Cardin, A. D. & Weintraub, H. J. R. (1989). *Arteriosclerosis*, **9**, 21–32.

Carrell, R. W. & Gooptu, B. (1998). *Curr. Opin. Struct. Biol.* **8**, 799–809.

Caughey, B., Brown, K., Raymond, G. J., Katzenstein, G. E. & Thresher, W. (1994). *J. Virol.* **68**, 2135–2141.

Clarke, L. A., Nasir, J., Zhang, H., McDonald, H., Applegarth, D. A., Hayden, M. R. & Toone, J. (1994). *Genomics*, **24**(2), 311–316.

Cudney, R., Patel, S., Weisgraber, K., Newhouse, Y. & McPherson, A. (1994). *Acta Cryst.* D**50**, 414–423.

Durand, P., Lehn, P., Callebant, I., Fabrega, S., Henrissat, B. & Mornon, J. P. (1997). *Glycobiology*, **7**, 277–284.

Grothe, R. (1999). Personal communication.

Guijarro, J. I., Sunde, M., Jones, J. A., Campbell, I. D. & Dobson, C. M. (1998). *Proc. Natl Acad. Sci. USA*, **95**, 4224–4228.

Hamazaki, H. (1987). *J. Biol. Chem.* **262**, 1456–1460.

Heegaard, N. H. H., Heegard, P. M. H., Roepstorff, P. & Robey, F. A. (1996). *Eur. J. Biochem.* **239**, 850–856.

Helms, L. R. & Wetzel, R. (1996). *J. Mol. Biol.* **257**, 77–86.

Jackson, R. L., Busch, S. J. & Cardin, A. D. (1991). *Physiol. Rev.* **71**, 481–539.

Jancarik, J. & Kim, S.-H. (1991). *J. Appl. Cryst.* **24**, 409–411.

Jiang, X., Myatt, E., Lykos, P. & Stevens, F. J. (1997). *Biochemistry*, **36**, 13187–13194.

Kakkis, E. D., Matynia, A., Jonas, A. J. & Neufeld, E. F. (1994). *Protein Expr. Purif.* **5**, 225–232.

Kakkis, E., Muenzer, J., Tiller, G., Waber, L., Belmont, J., Passage, M., Izykowski, B., Phillips, J., Walot, I., Doroshow, R., Hoft, R., Yu, K. T., Okazaki, S., Lewis, D., Lachman, R. & Neufeld, E. F. (1998). *Am. J. Hum. Genet.* **63**, 128.

Klunk, W. E., Pettegrew, J. W. & Abraham, D. J. (1989*a*). *J. Histochem. Cytochem.* **37**, 1273–1281.

Klunk, W. E., Pettegrew, J. W. & Abraham, D. J. (1989*b*). *J. Histochem. Cytochem.* **37**, 1293–1297.

Li, X. A., Hatanaka, K., Guo, L., Kitamura, Y. & Yamamoto, A. (1994). *Biochim. Biophys. Acta*, **1201**, 143–148.

Liu, Y., Hart, P. J., Schlunegger, M. P. & Eisenberg, D. S. (1998). *Proc. Natl Acad. Sci. USA*, **95**, 3437–3442.

McPherson, A. (1982). *Preparation and Analysis of Protein Crystals*, p. 76. New York: John Wiley & Sons.

Margalit, H., Fischer, N. & Ben-Sasson, S. A. (1993). *J. Biol. Chem.* **268**, 19228–19231.

Moriarty, D. F. & Raleigh, D. P. (1999). *Biochemistry*, **38**, 1811–1818.

Multhaup, G., Bush, A. I., Pollwein, P., Masters, C. L. & Beyreuther, K. (1992). *J. Protein Chem.* **11**, 398–399.

Nielsen, E. H., Sorensen, I. J., Vilsgaard, K., Andersen, O. & Svehag, S. E. (1994). *Acta Pathol. Microbiol. Immunol. Scand.* **102**, 420–426.

Neufeld, E. F. & Muenzer, J. (1989). *The Metabolic Basis of Inherited Disease*, 6th ed., edited by C. R. Scriver, A. L. Beaudet, W. S. Sly & D. Valle, pp. 1565–1587. New York: McGraw Hill.

Pepys, M. B. & Butler, P. J. G. (1987). *Biochem. Biophys. Res. Commun.* **148**, 308–313.

Phillips, F. C. (1962). *An Introduction to Crystallography*, 2nd ed., pp. 274–294. London: Longmans.

Puchtler, H., Sweat, F. & Levine, M. (1962). *J. Histochem. Cytochem.* **10**, 355–364.

Rossjohn, J., Cappai, R., Feil, S. C., Henry, A., McKinstry, W. J., Galatis, D., Hesse, L., Multhaup, G., Beyreuther, K., Masters, C. L. & Parker, M. W. (1999). *Nature Struct. Biol.* **6**, 327–331.

Sando, G. N. & Neufeld, E. F. (1977). *Cell*, **12**, 619–627.

Scott, H. S., Anson, D. S., Orsborn, A. M., Nelson, P. V., Clements, P. R., Morris, C. P. & Hopwood, J. J. (1991). *Proc. Natl Acad. Sci. USA*, **88**, 9695–9699.

Shapiro, L. J., Hall, C. W., Leder, I. G. & Neufeld, E. F. (1976). *Arch. Biochem. Biophys.* **172**, 156–161.

Sipe, J. D. (1992). *Annu. Rev. Biochem.* **61**, 947–975.

Small, D. H., Nurcombe, V., Reed, G., Clarris, H., Moir, R., Beyreuther, K. & Masters, C. L. (1994). *J. Neurosci.* **14**(4), 2117–2127.

Stoltzfus, L. J., Sosa-Pineda, B., Moskowitz, S. M., Menon, K. P., Dlott, B., Hooper, L., Teplow, D. B., Shull, R. M. & Neufeld, E. F. (1992). *J. Biol. Chem.* **267**(10), 6570–6575.

Sunde, M., Serpell, L. C., Bartlan, M., Fraser, P. E., Pepys, M. B. & Blake, C. C. F. (1997). *J. Mol. Biol.* **273**, 729–739.

Watson, D. J., Lander, A. D. & Selkoe, D. J. (1997) *J. Biol. Chem.* **272**, 31617–31624.

Westermark, P., Engstrom, U., Johnson, K. H., Westermark, G. T. & Betsholtz, C. (1990). *Proc. Natl Acad. Sci. USA*, **87**, 5036–5040.

Wood, S. J., Maleeff, B., Hart, T. & Wetzel, R. (1996). *J. Mol. Biol.* **256**, 870–877.